OPEN

# New MYC IHC Classifier Integrating Quantitative Architecture Parameters to Predict *MYC* Gene Translocation in Diffuse Large B-Cell Lymphoma

*Gilbert Bigras, MD, PhD,* Wei-Feng Dong, MD, PhD,* Sarah Canil, BSc,* Raymond Lai, MD, PhD,* Didier Morel, PhD,† Paul E. Swanson, MD,‡ and Iyare Izevbaye, MD, PhD§*

**Abstract:** A new automated MYC IHC classifier based on bivariate logistic regression is presented. The predictor relies on image analysis developed with the open-source ImageJ platform. From a histologic section immunostained for MYC protein, 2 dimensionless quantitative variables are extracted: (a) relative distance between nuclei positive for MYC IHC based on euclidean minimum spanning tree graph and (b) coefficient of variation of the MYC IHC stain intensity among MYC IHC-positive nuclei. Distance between positive nuclei is suggested to inversely correlate *MYC* gene rearrangement status, whereas coefficient of variation is suggested to inversely correlate physiological regulation of MYC protein expression. The bivariate classifier was compared with 2 other MYC IHC classifiers (based on percentage of MYC IHC positive nuclei), all tested on 113 lymphomas including mostly diffuse large B-cell lymphomas with known *MYC* fluorescent in situ hybridization (FISH) status. The bivariate classifier strongly outperformed the "percentage of MYC IHC-positive nuclei" methods to predict *MYC*+ FISH status with 100% sensitivity (95% confidence interval, 94-100) associated with 80% specificity. The test is rapidly performed and might at a minimum provide primary IHC screening for *MYC* gene rearrangement status in diffuse large B-cell lymphomas. Furthermore, as this bivariate classifier actually predicts "permanent overexpressed MYC protein status," it might identify non-translocation-related chromosomal anomalies missed by FISH.

Received for publication January 4, 2016; accepted February 29, 2016.

From the Departments of *Laboratory Medicine and Pathology, Cross Cancer Institute; §Laboratory Medicine and Pathology, Molecular Pathology Division, University of Alberta, Edmonton; ‡Department of Pathology and Laboratory Medicine, University of Calgary, Calgary, AB, Canada; and †Becton Dickinson, Office of Science, Medicine and Technology, Corporate Clinical Development, Pont-de-Claix, France.

The authors declare no conflict of interest.

Reprints: Gilbert Bigras, MD, PhD, FRCPC, Department of Laboratory Medicine and Pathology, Cross Cancer Institute, University of Alberta, 11560 University Ave NW, Edmonton, AB, Canada T6G 1Z2 (e-mail: gilbert.bigras@ahs.ca). Software available at https://github.com/gilbertbigras/MYC-IHC



**Key Words:** MYC, IHC, Burkitt lymphoma, DLBCL, image analysis, minimum spanning tree graph

(*Appl Immunohistochem Mol Morphol* 2018;26:54–63)

MYC is the master regulator of nearly all important cellular functions, especially growth regulation and cellular metabolism.[1] As of 2003, an integrated database[2] of genes responsive to *MYC* transcription factors had 647 entries clustered in different functional groups, including 120 genes related to metabolism, 82 related to protein synthesis, 25 associated with cell cycle control, and 5 involved in DNA replication. Cell division requires considerable metabolic support and the importance of *MYC* is illustrated by its ability to coordinate both. *MYC* was initially identified as an oncogene with the demonstration of the reciprocal translocation between *MYC* and immunoglobulin heavy loci t(8;14)(q24;q32) (MYC+) in Burkitt lymphoma.[3,4] In recent years, different reports have demonstrated *MYC*+ in a small subset (3% to 16%) of diffuse large B-cell lymphomas (DLBCL).[5] When *MYC*+ is associated with another translocation such as *BCL2* t(14;18)(q32;q21) (*BCL2*+), the involved DLBCL is labeled as double hit (DH). DH (*MYC*+/*BCL2*+) prevalence is also imprecise and varies between 0% and 12% in recent studies.[5] Synergistic action of *MYC*+ and *BCL2*+ confers a dismal outcome[5–9] and requires more aggressive therapy. DH also refers to other associations, such as *MYC*+ and *BCL6* t(3;16)(q27;p11) (*BCL6*+), which also predicts a dismal outcome.[10] Rare triple-hit B-cell lymphomas (*MYC*+/*BCL2*+/*BCL6*+) are also reported.[11]

Currently, *MYC*+ is assessed with fluorescent in situ hybridization (FISH). There are 2 different FISH approaches to detect *MYC* rearrangement, which are the dual-fusion and the break-apart techniques. The former is less sensitive to detect *MYC*+ especially when the translocation involves a non-IGH partner; the latter detects *MYC*+ independently of the translocation partner. The break-apart technique might, however, miss cryptic rearrangements that should be detected by the dual-fusion technique. Consequently, utilization of both techniques may increase *MYC*+ detection sensitivity.[12] There are other mechanisms that convey MYC protein overexpression in DLBCL: *MYC* gene amplification[13] and

micro-RNA alteration[14,15] are relatively frequent alterations. Whereas amplification can be detected by FISH (ideally pending specific probes[16]), micro-RNA alteration is not. Nonetheless, these dysregulated *MYC* DLBCL, not associated with chromosomic translocation, appear to be associated with similar negative clinical implications.[17] Therefore, the utilization of MYC IHC might be an alternative to FISH: actually, many investigations, assessing the percentage of nuclei IHC positive for MYC protein, have concluded that MYC IHC is capable of predicting *MYC*+.[7,18–21] These studies, however, report a variety of thresholds (30%, 40%, and 50%) to predict *MYC*+. Of interest, in at least 2 studies,[18,22] authors warn readership about potential interobserver and intraobserver variations in MYC IHC scoring, especially when the IHC stain shows heterogeneity. These observations are the basis of the current work wherein we suggest a new approach to MYC IHC assessment. The aforementioned crucial roles of *MYC* in cellular growth and metabolism require tight regulation of *MYC* gene expression to maintain cellular homeostasis. Among safeguard mechanisms, both *MYC* mRNA and MYC protein have short life (~30 min for the protein) which are effective means of gene regulation.[1,23] It is hypothesized that persistence and loss of *MYC* gene regulation are, respectively, associated with modulated and constant protein expression with observable IHC architectural modifications. First, the amount of MYC protein per nucleus depends on *MYC* regulation: in permanently upregulated *MYC* neoplasms, the MYC IHC stain is expected to be strong and, more important, similar among all malignant nuclei; the opposite situation is regulated *MYC* expression, wherein both spatial and temporal variation in MYC IHC stain reflect physiological cycling of MYC. Hence, MYC stain variability is hypothesized to be proportional to *MYC* gene regulation. Second, the spatial distribution of MYC IHC-positive nuclei is regulation dependent: in permanently upregulated *MYC* neoplasms, positive MYC IHC nuclei appear gregarious or "clonal"; in regulated MYC neoplasms, positive nuclei are randomly scattered among negative ones reflecting persistence of normal regulation patterns within the tissue. Relative distance between positive *IHC* MYC nuclei is thus hypothesized to be proportional to gene regulation (Fig. 1). Combined stain variability and relative distance between MYC IHC-positive nuclei will be compared with the currently used "percentage of positive IHC MYC nuclei" to predict *MYC*+.

## METHODOLOGY

### Dimensionless Variables as Predictors of MYC Gene Status

Coefficient of variation (CV = $\sigma/\nu$) of MYC IHC stain intensity is defined as the division of the SD ($\sigma$) of stain intensity by the mean ($\nu$) of IHC stain intensity measured in MYC IHC-positive nuclei. CV and $\sigma$ are both measurements of dispersion, but the former has the advantage to be dimensionless. Relative distance between positive MYC IHC nuclei is obtained by utilizing a second dimensionless variable defined as the division of the average distance between positive IHC MYC nuclei by the average distance between all nuclei. Distance between nuclei is the distance between closest neighbor. This latter is obtained with the utilization of euclidean minimum spanning tree[24] (EMST), which provides for each nucleus

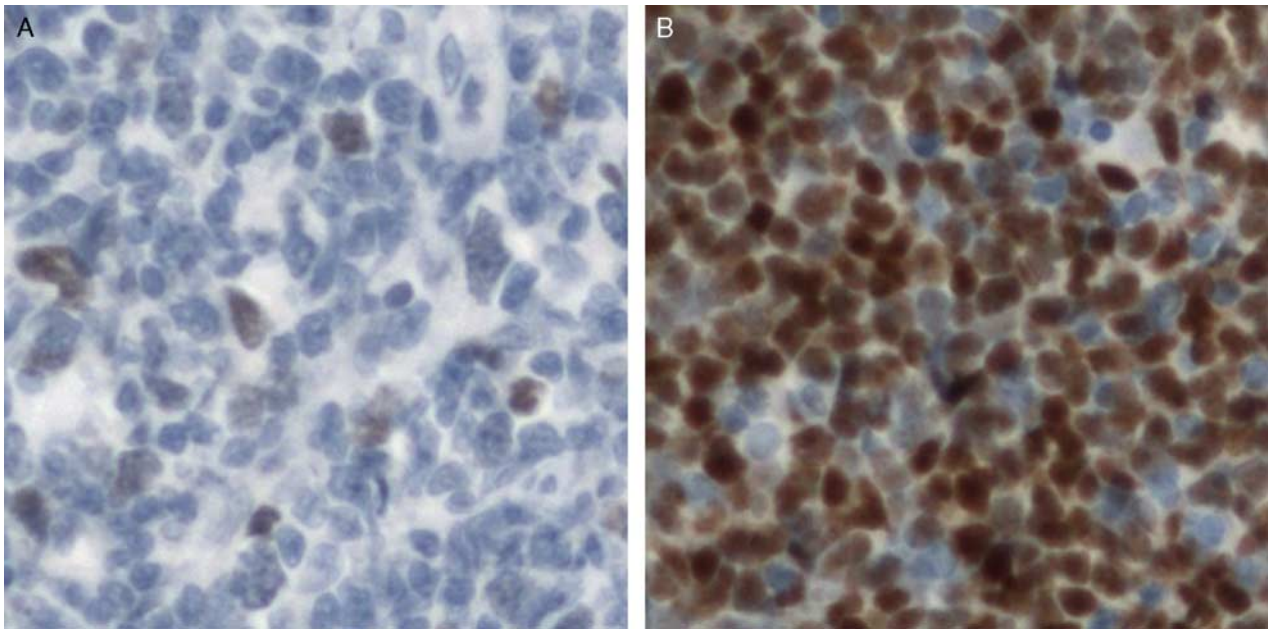


**FIGURE 1.** A, DLBCL *MYC*− with scattered positive MYC IHC nuclei and variable stain intensity. B, DLBCL *MYC*+ with gregarious positive MYC IHC nuclei and less variable stain intensity. Both distance between positive nuclei and stain variability are hypothesized to be directly proportional to *MYC* gene regulation (Fig. 2).

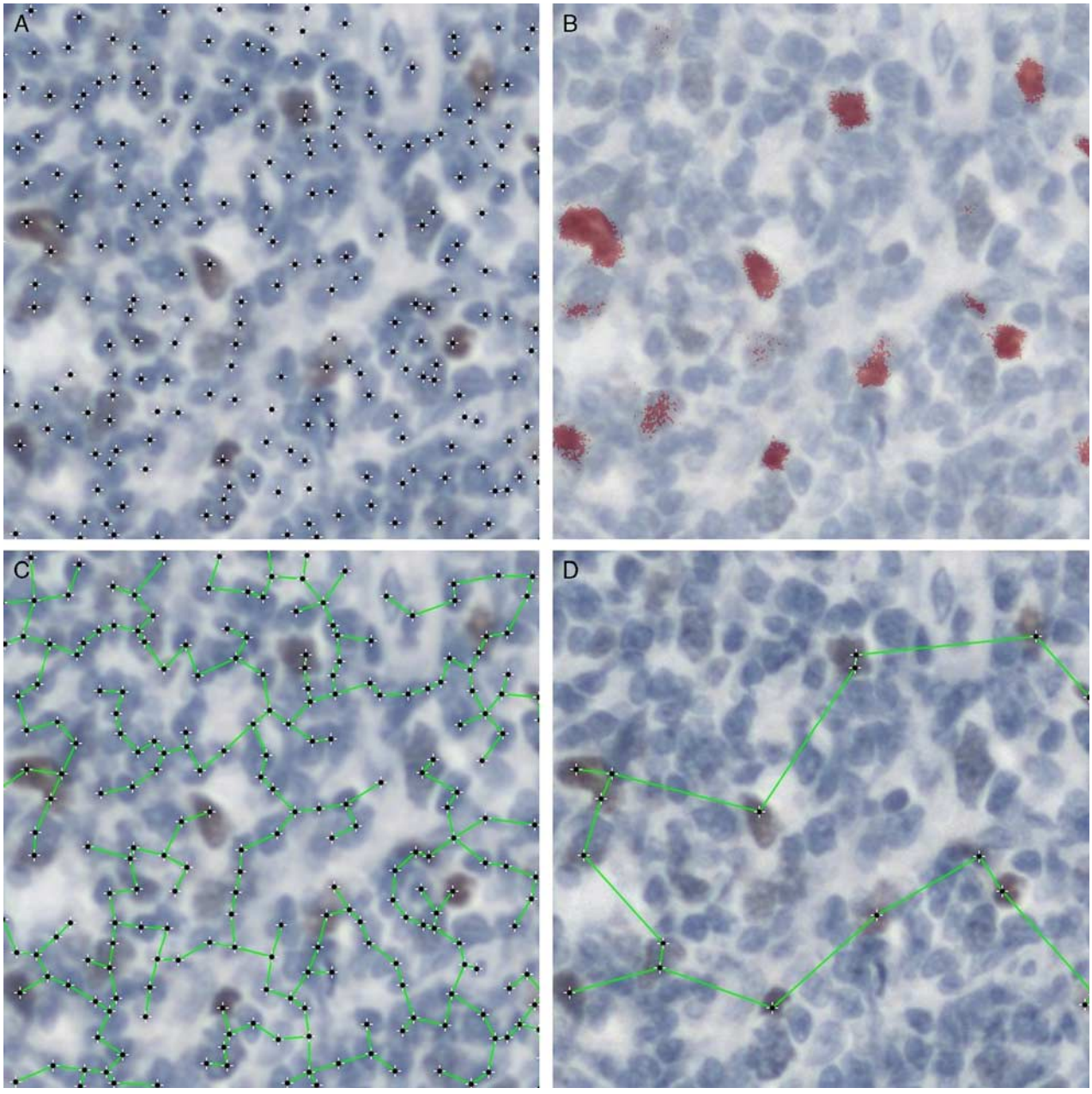


**FIGURE 2.** The 4 pictures represent the same MYC IHC preparation (DLBCL). (A) Detection of nuclei using "find maxima" algorithm, (B) superimposed threshold image of DAB component (red), (C) euclidean minimum spanning tree (all nuclei), (D) euclidean minimum spanning tree (positive MYC IHC nuclei). CV of stain intensity is measured in positive MYC IHC nuclei and ratio EMST computed from division of "average edge length" from D over "average edge length" from C. full color online

the distance of the closest neighbor. EMST is assessed twice: first for positive MYC IHC nuclei only and a secondly for all nuclei. A ratio EMST is then computed by dividing the former EMST by the latter. The larger ratio EMST, the larger the number of MYC IHC myc negative nuclei intercalated between positive ones. CV and ratio EMST are the 2 suggested dimensionless and independent variables which will be used to predict the categorical-dependent variable "*MYC* gene rearrangement status."

## MYC IHC

IHC was performed on 4 μm formalin-fixed paraffin-embedded tissues sections that were baked for 1 hour at 60°C. Slides were stained using the Ventana XT platform and Optiview detection kit (760-700; Ventana Medical Systems Inc., Tucson, AZ) after retrieval with CC1 (pH 8.5) for 72 minutes. A rabbit monoclonal anti-MYC (1/50, EP121, 395R-15; Cell Marque, Rocklin, CA) was incubated for 40 minutes at 37°C. Slides were counterstained using

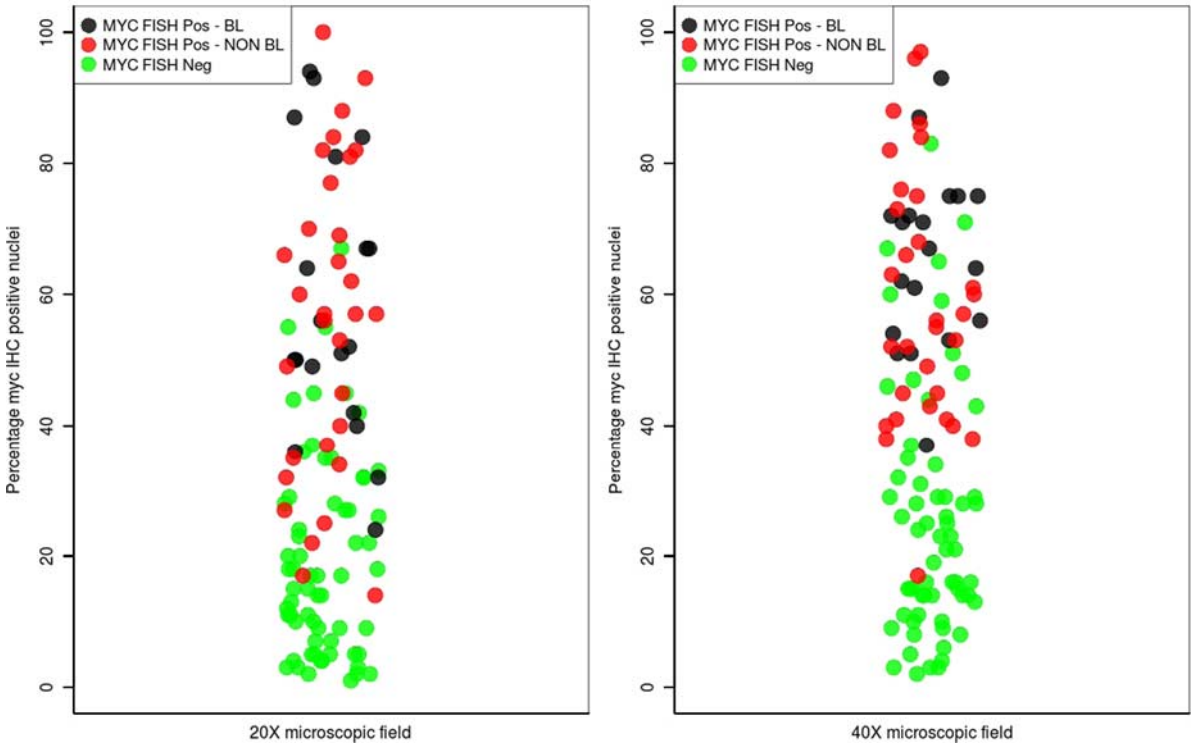


**FIGURE 3.** Stripcharts illustrating 113 lymphomas (mostly DLBCL) according to percentage of MYC IHC-positive nuclei and MYC gene rearrangement status. (A) ×20 microscopic objective and (B) ×40 microscopic objective. Results obtained by automatic image analysis. In both situations the higher the percentage of positive nuclei, the higher the probability of MYC+ detected by FISH. Among MYC+ cases, there is no obvious difference between BL and NON BL. full color online

Gill's Hematoxylin (380150; Leica Biosystems, Richmond, IL) for 15 seconds. An onslide control consisting of BL (MYC+), DLBCL (MYC−), and melanoma was used to ensure consistent staining in and between staining runs.

## Image Acquisition, Analysis, and Algorithm Description

Image analysis was performed using the ImageJ[25] platform, a public domain, Java-based image processing program developed at the National Institutes of Health (Bethesda, MD). To get CV and ratio EMST, 1 pathologist (G.B.) digitized 1 field on each of the 113 MYC IHC slides using a ×20 objective targeting the visually most intensely stained area. To get percentages of MYC IHC-positive nuclei, another pathologist (W.-F.D.) digitized 2 fields from each of the same 113 slides using ×20 and ×40 objectives and again targeting the visually most intensely stained area. Two different microscopes were utilized: (G.B.) Nikon Eclipse E600 microscope, 0.25 aperture (×20) and 0.65 (×40) and (W.-F.D.) Nikon Eclipse 80i microscope, 0.5 aperture (×20) and 0.75 (×40) (Nikon Instruments Inc., Melville, NY). Both microscopes are equipped with a QImaging Micropublisher 5.0 RTV camera (QImaging Corp., Surrey, BC), which uses a Sony ICX282 progressive scan interline CCD producing 24-bit color pictures with a resolution of 2560×1920 pixels. For all images, a priori background correction[26] was applied. Percentage of positive MYC IHC nuclei were computed with Immunoratio,[27] an open source software based on the ImageJ platform. CV and ratio EMST were computed using an in-house developed algorithm (G.B.) using combination of ImageJ macros and plugins. In summary, for each MYC IHC image, a "find maxima" algorithm provides $(x,y)$ coordinates (centroids) of all nuclei (Fig. 2A); color deconvolution[28] plugin isolates DAB staining which permits identification of positive nuclei (Fig. 2B); a first EMST is built with centroids from all nuclei (Fig. 2C) and a second EMST is built with centroids from positive MYC IHC nuclei (Fig. 2D). DAB intensity is measured in positive nuclei averaging 9 samples per nucleus from a 3×3 matrix whose center is the centroid $(x,y)$. Finally, CV is computed from all measured DAB intensities in positive MYC IHC nuclei.

## Case Selection

A total of 113 lymphomas (19 BL, 77 DLBCL, 6 intermediate between BL and DLBCL, and 11 unclassified aggressive B-cell lymphomas) diagnosed between 2010 and 2015 with known *MYC* status were

selected. MYC IHC stains were produced in 2014 and 2015. All specimens had been fixed in formalin (37% formaldehyde in aqueous solution) and embedded in paraffin. Although a small group of cases (~20%) was studied retrospectively, all cases in this analysis were stained utilizing freshly cut thin sections.

## Interphase MYC FISH Analysis

A nuclear preparation was made from paraffin-embedded tissue. Two 20 µm curls (contiguous to sections used for IHC) were cut from paraffin block. The curls were deparaffinized, hydrated in ethanol, digested in 10% proteinase K, washed, and the resulting nuclear suspension deposited onto glass slides. FISH was performed with the VYSIS LSI *MYC* Dual Color Break-apart rearrangement probe set (Abbott Molecular, Des Plaines, IL) that hybridizes to the band region 8q24. This probe detects the most prevalent translocation t(8;14)(q24;q32)*IGH-MYC* involving the heavy-chain immunoglobulin locus but also detects 2 additional variants t(2;8)(p11.2;q24.1)*IGK-MYC* and t(8;22)(q24.1;q11.2)*IGL-MYC* involving light-chain immunoglobulin loci. The established normal cutoff for a positive result is 10% of the cells showing an abnormal signal pattern. Appropriate negative and positive controls were used. An average of 100 interphase nuclei were examined independently by 2 observers using an Olympus Provis microscope system on ×1000 magnification.

## MYC IHC Stain and Variables Predictors Stability

Immunohistochemistry technique relies on numerous preanalytical and analytical variables that influence the immunoreactivity of proteins. As some antibodies require freshly diluted antibody or freshly cut unstained slides, the stability of MYC antibody dilution over 6 weeks was verified as well as antigen preservation within unstained thin section over time. The same onslide controls [1 BL (*MYC*+) and 1 DLCBL (*MYC*−)] were simultaneously submitted to variable preanalytical conditions including incremental delay after block sectioning, various aging antibody dilution, or combination of both. The goal was to see whether the MYC IHC stain would remain stable within a timeframe of 6 weeks, and if not, to measure the influence, if any, of stain variability on ratio EMST, CV, and percentage of positive MYC IHC nuclei.

## Statistical Analysis

Statistical analysis and statistical figures were created using R language[29] (version 3.2.2; R Foundation, Vienna). To predict *MYC* gene rearrangement, simple logistic regression model was individually applied on the 2 variables: percentage ×20 and percentage ×40; multiple logistic regression was applied to the bivariate (CV, ratio EMST). To estimate how accurate the 3 models would perform, an exhaustive cross-validation[30] (Leave-one-out cross-validation) was applied to each model. The statistical null hypothesis is

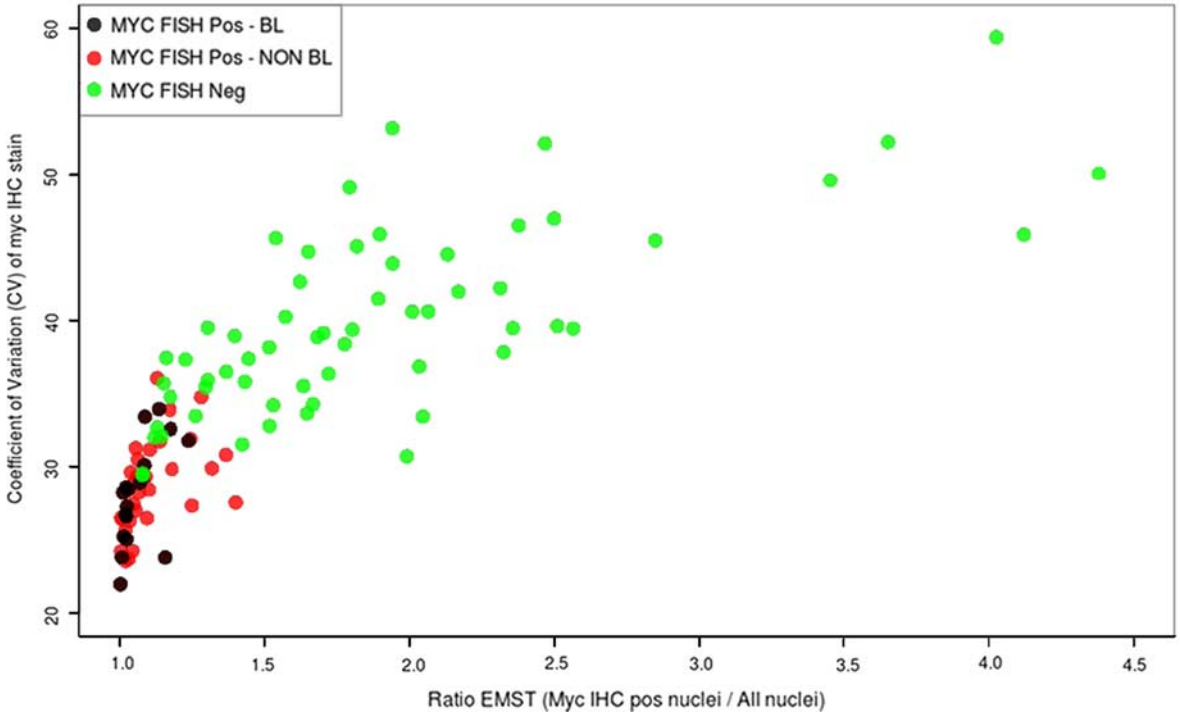


**FIGURE 4.** Scatterplot illustrating 113 lymphomas (mostly DLBCL) according to ratio EMST against CV of MYC IHC stain among positive MYC IHC nuclei. Segregation of MYC+ and MYC− (assessed by FISH) is evident. The higher ratio EMST and CV, the higher the probability of MYC status to be negative. Among MYC+ cases, there is no obvious difference between BL and NON BL. full color online

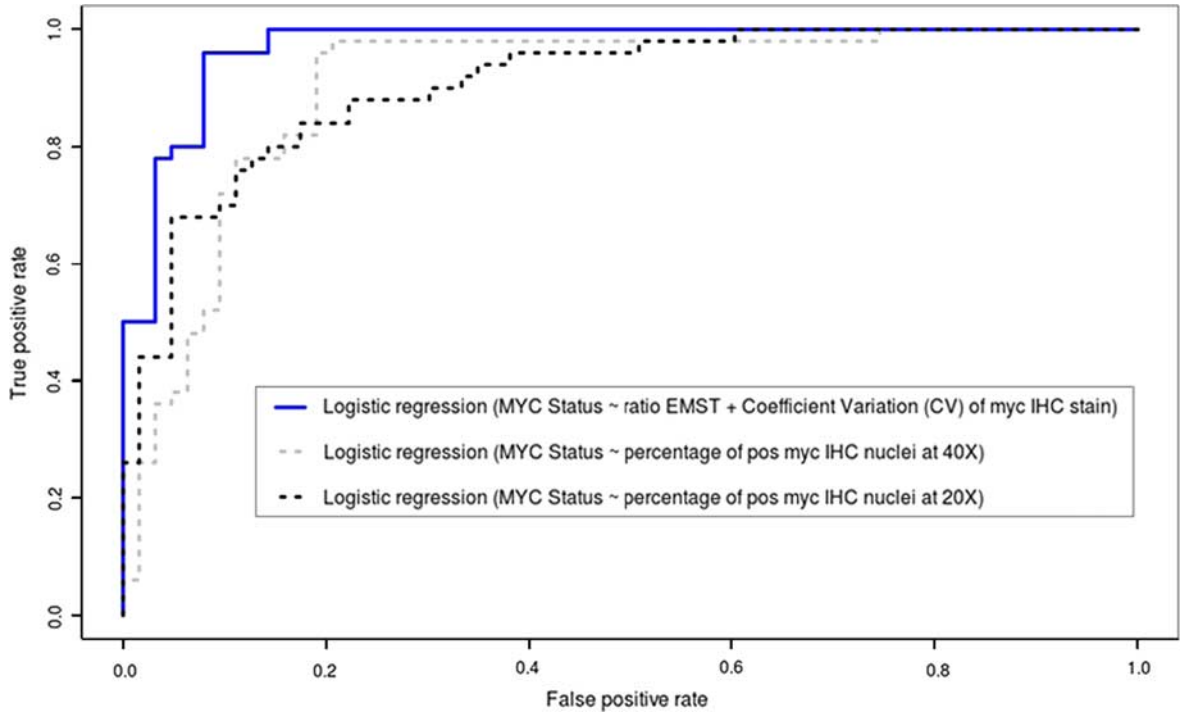


**FIGURE 5.** Receiver operating characteristics curves of the 3 logistic regression models built with Leave-one-out cross-validation. Multivariate logistic regression is associated with the highest area under the curve (AUC = 97.1%). Simple logistic regression models $\times 40$ and $\times 20$ ROC area under the curve values are, respectively, 90.6% and 90.5%. full color online

that the probability of $MYC+$ is not associated with the aforementioned variables. Statistical significance was evaluated with Wald $Z$-statistic test. Performance of predictors was assessed with receiver operating characteristic (ROC) and accuracy performance using the ROCR package.[31] To compare ROC curves of the 3 different predictors and to measure the confidence intervals (CI) of sensitivity and specificity, the pROC R package was utilized.[32] CI assessment relied on 2000 stratified bootstrap replicates. A $P$-value of $\leq 0.05$ was selected as the level of significance in all analyses. Figure 2 was created with the FigureJ plugin.[33] This study was approved by the Alberta Cancer Research Ethics Committee (file CC-15.0247).

## RESULTS

### Predictive Capacity of Variables

Fifty cases were $MYC+$ (19 BL, 21 DLBCL, and 10 others) and 63 were $MYC-$ (0 BL, 56 DLBCL, and 7 others) by FISH. For each predictor, computation of individual variables took $<2$ minutes. Descriptive statistics of the total number of harvested nuclei per case are: mean (3105), median (3022), first quartile (2349), third quartile (3768), and range (1266 to 5945). $MYC$ gene rearrangement classification of the 113 cases is illustrated in Figures 3 and 4, where visual separation of $MYC+$ and $MYC-$ is obvious for all predictive models. The null hypothesis is rejected: in all logistic regression analyses, all variables were statistically significant ($< 0.05$). For the 3 models, probability of $MYC+$ are, respectively, computed as follows:

$$\frac{1}{1+e^{-(-3.6676+0.09668\times \%20X)}},$$

$$\frac{1}{1+e^{-(-4.2325+0.09932\times \%40X)}},$$

and

$$\frac{1}{1+e^{-(24.267-6.2209\times \text{ratioEMST}-0.5053\times \text{CV})}}.$$

If all 3 models can predict $MYC$ status, visual inspection suggests that the multiple logistic regression using bivariate (ratio EMST, CV) is superior than individual simple logistic models. Superiority of bivariate model is confirmed by inspecting superimposed ROC curves (Fig. 5), where areas under the curve are 97.1% (95% CI, 0.95-0.99), 90.6 (95% CI, 0.85-0.96), and 90.5 (95% CI, 0.85-0.96) for, respectively (ratio EMST, CV), $\times 40$ and $\times 20$. Inspection of curves of test accuracy and associated density distribution of $MYC+$ and $MYC-$ clearly shows the superiority of the multiple logistic regression model (Fig. 6).

Figure 7 illustrates the expected sensitivities and specificities of the 3 predictive models obtained by selecting different cutoffs. These results are in line with previous figures. The multivariate logistic regression model shows the possibility to maintain a virtual 100% sensitivity associated with strong specificity: choosing the

 

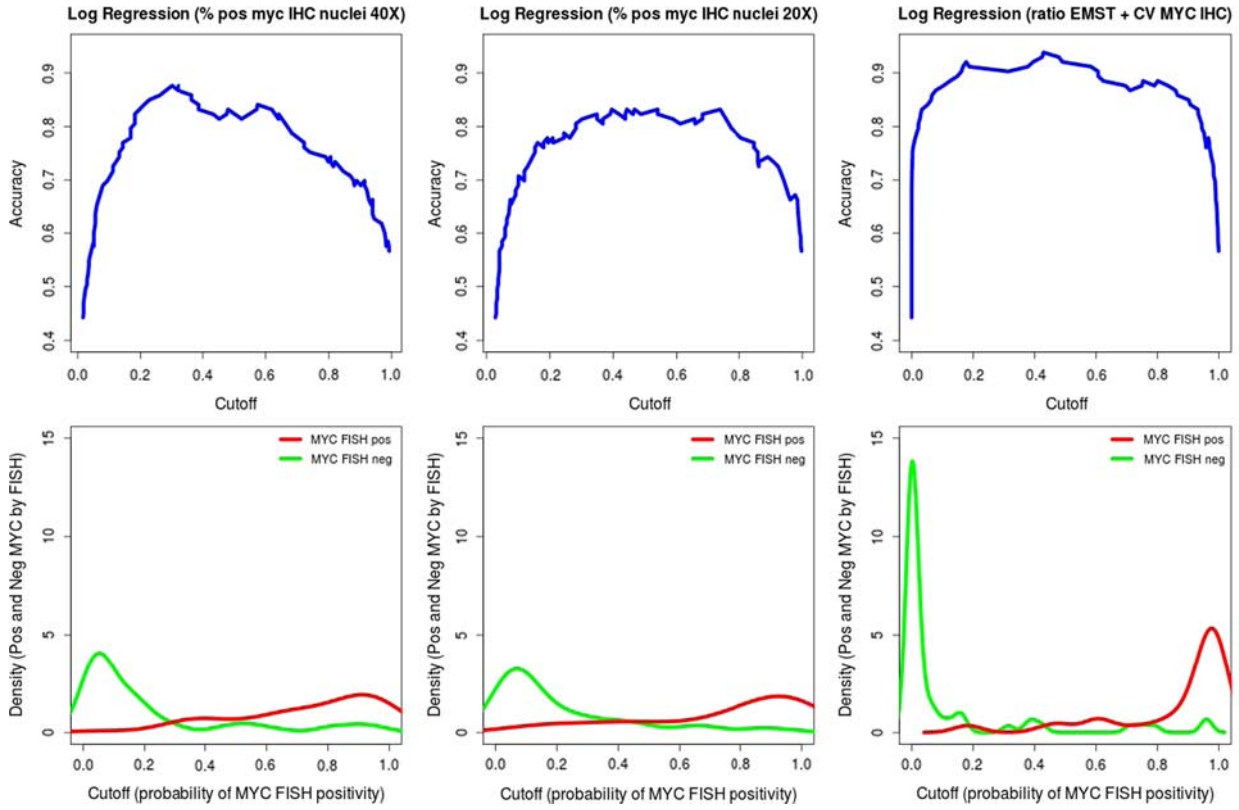


**FIGURE 6.** Upper charts illustrate accuracy of individual predictive models and lower charts corresponding histogram distribution of MYC+ and MYC− subsets identified by FISH. For all charts, the horizontal axis corresponds to probability for a case to be MYC+ (from 0 to 1) as computed by logistic regression. Multivariate logistic regression based on ratio EMST and CV shows the strongest accuracy well explained by the chart below where MYC+ (red) and MYC− (green) are clearly separated. full color online

cutoff of 11% of probability, the associated sensitivity and specificity are 100% (95% CI, 94%-100%) and 80 (95% CI, 76%-95%). The 2 other simple logistic regressions models can have 100% sensitivity but only with the cost of a much lower specificity.

## MYC IHC Stain and Variables Predictors Stability

Stain intensity drop was found to be proportional to ages of both antibody dilution and unstained tissue section. Both freshly prepared antibody dilution and freshly cut thin section are required to maintain constant high MYC IHC stain intensity over time. Of interest, the extent of stain variability depends on the amount of MYC antigen within the tissue. For the *MYC*+ control, the average stain intensity per nucleus varies approximately in a range of 1:1.5 (Fig. 8A, *y*-axis); for the *MYC*− control, the average stain intensity per nucleus varies approximately in a range of 1:7.5 (Fig. 8B, *y*-axis). Computed predictors variables vary differently: for the *MYC*+ control, percentage of positive MYC IHC nuclei, CV, and ratio EMST are stable and are barely influenced by stain intensity (Fig. 8A, *x*-axis).In contrast, for the *MYC*− control, percentage of positive MYC IHC nuclei varies with stain intensity, whereas CV and ratio EMST remain relatively stable (Fig. 8B, *x*-axis).

## DISCUSSION

A new MYC IHC classifier to predict *MYC* gene rearrangement status in DLBCL using the dimensionless variables ratio EMST and CV is presented. On the basis of automated image analysis, this classifier provides fast assessment with potentially minimal interobserver variability. Careful inspection of Figure 2A shows that centroid detection by the "find maxima" algorithm is reasonably precise, but not perfect: with thousands of nuclei harvested by the algorithm, the test has shown statistical power. The choice of dimensionless variables (ratio EMST and CV) should allow for the production of comparable results independent of the utilized image analysis/microscope environment.

In order for this classifier to partially replace or supplement FISH by triaging DLBLC, the test would need to meet class II biomarker requirements. The reproducibility of the MYC IHC assay used in this study requires freshly prepared antibody dilution and freshly cut unstained slides. Hence, it might then also be necessary to define preanalytical guidelines (similar to those described for the consistent performance of biomarker IHC in breast cancer[34,35] that ideally ensure reliable hormone receptor results between laboratories). This new MYC IHC classifier integrates 2 independent variables that are based on IHC stain variability (CV) and morphologic data. It was

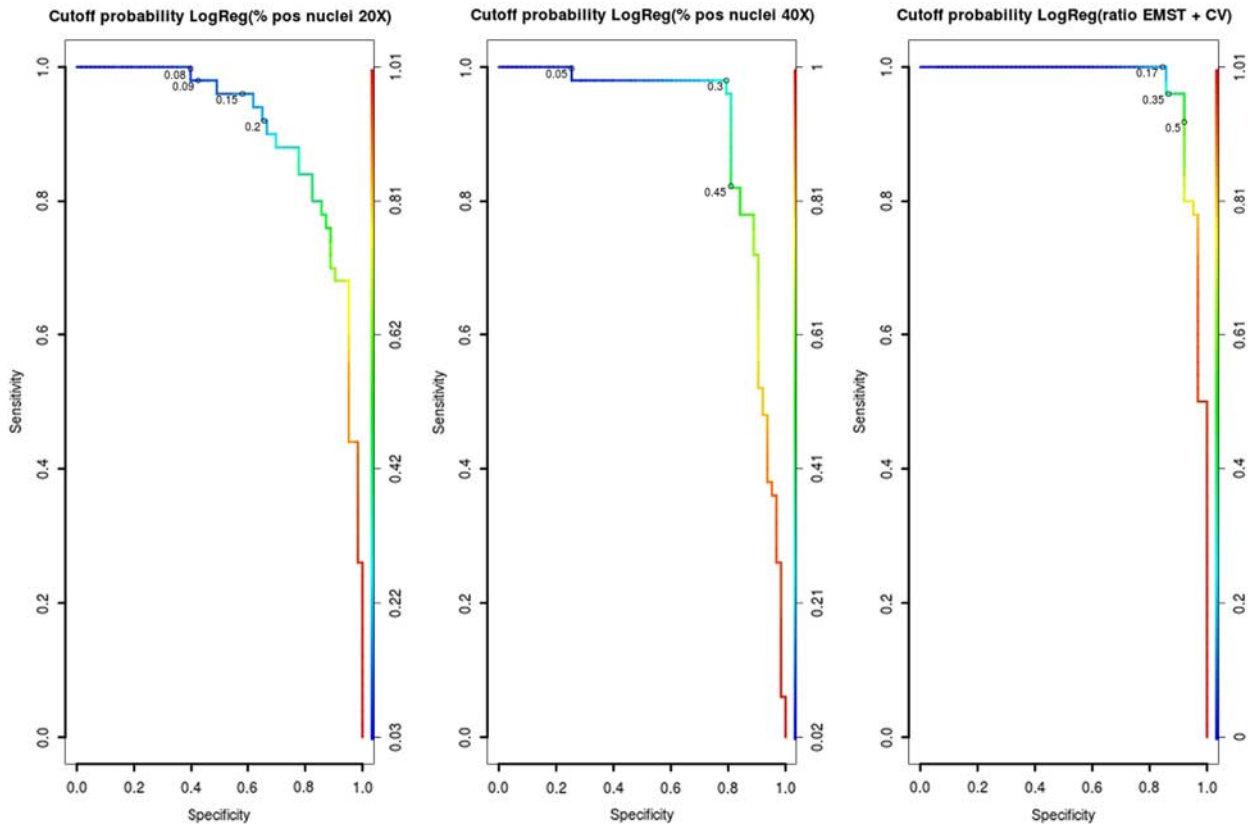


**FIGURE 7.** Receiver operating characteristics curves of the 3 logistic regression models (similar to Fig. 5) with cutoff probabilities: for the 3 models, it is possible to determine a cutoff probability with 100% sensitivity. For the ×20, ×40, and bivariate (ratio EMST, CV) these cutoffs are, respectively, 8%, 5%, and 17%. The associated specificities are, however, significantly different and are approximately 40%, 25%, and 85%. full color online

suggested that CV is a measure of the maintenance of physiological cycling protein expression. The integration of IHC information with a quantitated architecture parameter is thought to explain the superior classification capacity compared with currently used assessments based on the percentage of MYC IHC-positive nuclei alone. As suggested by one of the reviewer of this manuscript, careful documentation of lymphomas with unusual IHC staining, for instance heterogenous MYC staining, should be documented with both IHC and FISH techniques. Furthermore, reproducibility of this method should be demonstrated in other laboratories: to this end, the software is available from the Web site GitHub: https://github.com/gilbertbigras/MYC-IHC.

This paper also suggests that CV and ratio EMST are more robust variables than percentage of MYC IHC-positive nuclei, especially when preanalytical conditions create IHC stain variability. CV robustness would be explained as follows: even if the average IHC stain intensity of nuclei varies (secondary to preanalytical conditions), stain intensity dispersion around a given average (measured by CV) would not, as every single nucleus stain intensity is shifted with the average. Furthermore, even if stain intensity variation directly influences the number of positive nuclei and consequently the percentage, the average edge length forming the EMST graph is not. It has been demonstrated that neoplastic 2D architecture can be quantified by different graphs such as EMST and Voronoi. Computed parameters derived from these graphs show stability after including a certain number of centroids.[36] This is particularly relevant for tissue with a small number of nuclei positive for MYC and/or low content of MYC antigen per nucleus (Fig. 8B, $MYC-$). With high content of MYC antigen per nucleus (Fig. 8A, $MYC+$), the preanalytical deficiencies do not affect the stability of variables.

If the classifier strongly predicts *MYC* gene rearrangement status, it would be more precise to suggest that it predicts permanent dysregulated MYC protein overexpression. Therefore, if a $MYC+$ status confers to a DLBLC a permanent dysregulated MYC protein overexpression, the opposite is not always true: as already discussed there are other molecular anomalies which are $MYC-$. This might explain the presence of some $MYC-$ (green circles) found in "positive" territory (Figs. 3, 4). If these cases are confirmed to be associated with dismal outcomes,[20] bivariate MYC IHC classifier might outperform FISH. New investigation should, however, also demonstrate that these cases are associated with molecular anomalies not related to chromosomal translocation.

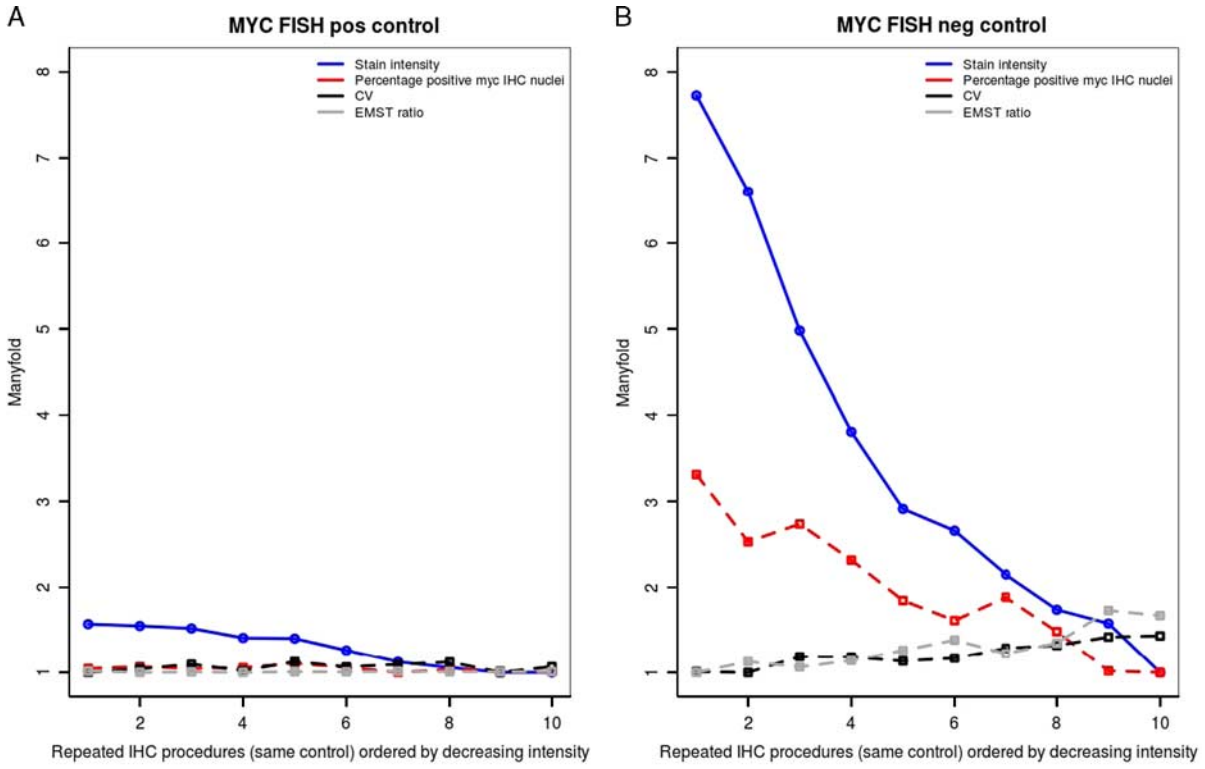


**FIGURE 8.** Ten repeated IHC procedures (*x*-axis) with different preanalytical conditions (explained in the Methodology section) performed simultaneously on 2 controls (A and B) placed on the same slides: (A) BL (MYC+) and (B) DLCBL (MYC−) against different variables (*y*-axis, manyfold). IHC procedures are ordered according to decreasing average MYC IHC stain intensities (blue lines) from left to right. Stain intensity variation is more significant when the amount of MYC antigen within the tissue is small (B); percentage of positive MYC IHC nuclei (red line) is then sensitive to stain intensity variability, whereas CV and ratio EMST (gray and black lines) remain more stable to the same stain variations (B). When the amount of MYC antigen within the tissue is high (A), all variables remain stable. full color online

In conclusion, we propose that this new IHC analytical method that combines IHC, image analysis, and graph theory could be utilized to triage DLCBL. Providing a probability cutoff of 11%, any DLBLC with a probability $<11\%$ could be considered *MYC*− and FISH would not be necessary. In contrast, any DLBLC with a probability $\geq 11\%$ should be investigated with FISH to confirm *MYC* gene rearrangement, with subsequent *BCL2* and *BCL6* FISH assessments to identify DH and/or triple-hit DLBLC. A significant number of patients could be safely triaged as *MYC*− at relatively low cost and with quick turnaround time.

## REFERENCES

1. Miller DM, Thomas SD, Islam A, et al. c-Myc and cancer metabolism. *Clin Cancer Res*. 2012;18:5546–5553.
2. Zeller KI, Jegga AG, Aronow BJ, et al. An integrated database of genes responsive to the Myc oncogenic transcription factor: identification of direct genomic targets. *Genome Biol*. 2003;4:R69.
3. Zech L, Haglund U, Nilsson K, et al. Characteristic chromosomal abnormalities in biopsies and lymphoid-cell lines from patients with Burkitt and non-Burkitt lymphomas. *Int J Cancer*. 1976;17:47–56.
4. Dalla-Favera R, Bregni M, Erikson J, et al. Human c-myc onc gene is located on the region of chromosome 8 that is translocated in Burkitt lymphoma cells. *Proc Natl Acad Sci*. 1982;79:7824–7827.
5. Aukema SM, Siebert R, Schuuring E, et al. Double-hit B-cell lymphomas. *Blood*. 2011;117:2319–2331.
6. Friedberg JW. Double hit diffuse large B-cell lymphomas: diagnostic and therapeutic challenges. *Chin Clin Oncol*. 2015;4:1–7.
7. Pfreundschuh M. Growing importance of MYC/BCL2 immunohistochemistry in diffuse large B-cell lymphomas. *J Clin Oncol*. 2012;30:3433–3435.
8. Li S, Lin P, Young KH, et al. MYC/BCL2 double-hit high-grade B-cell lymphoma. *Adv Anat Pathol*. 2013;20:315–326.
9. Lin P, Medeiros LJ. The impact of MYC rearrangements and 'double hit' abnormalities in diffuse large B-cell lymphoma. *Curr Hematol Malig Rep*. 2013;8:243–252.
10. Li S, Desai P, Lin P, et al. MYC/BCL6 double hit lymphoma (DHL): a tumor associated with an aggressive clinical course and poor prognosis. *Histopathology*. 2015. [Epub ahead of print] Doi:10.1111/his.12884.
11. Wang W, Hu S, Lu X, et al. Triple-hit B-cell lymphoma with MYC, BCL2, and BCL6 translocations/rearrangements: clinicopathologic features of 11 cases. *Am J Surg Pathol*. 2015;39:1132–1139.
12. Muñoz-Mármol AM, Sanz C, Tapia G, et al. MYC status determination in aggressive B-cell lymphoma: the impact of FISH probe selection. *Histopathology*. 2013;63:418–424.
13. Rao PH, Houldsworth J, Dyomina K, et al. Chromosomal and gene amplification in diffuse large B-cell lymphoma. *Blood*. 1998;92:234–240.
14. Lenz G, Wright GW, Emre NCT, et al. Molecular subtypes of diffuse large B-cell lymphoma arise by distinct genetic pathways. *Proc Natl Acad Sci*. 2008;105:13520–13525.

15. Leucci E, Cocco M, Onnis A, et al. MYC translocation-negative classical Burkitt lymphoma cases: an alternative pathogenetic mechanism involving miRNA deregulation. *J Pathol*. 2008;216: 440–450.
16. Ventura RA, Martin-Subero JI, Jones M, et al. FISH analysis for the detection of lymphoma-associated chromosomal abnormalities in routine paraffin-embedded tissue. *J Mol Diagn*. 2006;8: 141–151.
17. Stephens DM, Sweetenham JW. Clinical controversies of double-hit lymphoma. *Am J Hematol Oncol*. 2015;11:10–16.
18. Lynnhtun K, Renthawa J, Varikatt W. Detection of MYC rearrangement in high grade B cell lymphomas: correlation of MYC immunohistochemistry and FISH analysis [miscellaneous article]. *Pathology (Phila)*. 2014;46:211–215.
19. Kluk MJ, Chapuy B, Sinha P, et al. Immunohistochemical detection of MYC-driven diffuse large B-cell lymphomas. *PLoS One*. 2012;7:e33813.
20. Green TM, Young KH, Visco C, et al. Immunohistochemical double-hit score is a strong predictor of outcome in patients with diffuse large B-cell lymphoma treated with rituximab plus cyclophosphamide, doxorubicin, vincristine, and prednisone. *J Clin Oncol*. 2012;30:3460–3467.
21. Agarwal R, Lade S, Liew D, et al. Role of immunohistochemistry in the era of genetic testing in MYC-positive aggressive B-cell lymphomas: a study of 209 cases. *J Clin Pathol*. 2016;69:266–270. Doi:10.1136/jclinpath-2015-203002.
22. Mahmoud AZ, George TI, Czuchlewski D, et al. Scoring of MYC protein expression in diffuse large B-cell lymphomas: concordance rate among hematopathologists. *Mod Pathol*. 2015;28:545–551.
23. Hann SR, Eisenman RN. Proteins encoded by the human c-myc oncogene: differential expression in neoplastic cells. *Mol Cell Biol*. 1984;4:2486–2497.
24. Euclidean minimum spanning tree.2015. Available at: https://en.wikipedia.org/w/index.php?title = Euclidean_minimum_spanning_tree&oldid = 680080033. Accessed November 14, 2015.
25. Abramoff MD, Magalhães PJ, Ram SJ. Image processing with ImageJ. *Biophotonics Int*. 2004;11:36–42.
26. Landini G. How to correct background illumination in brightfield microscopy. 2014. Available at: http://imagejdocu.tudor.lu/doku.php?id = howto:working:how_to_correct_background_illumination_in_brightfield_microscopy&do = export_pdf. Accessed November 25, 2015.
27. Tuominen VJ, Ruotoistenmäki S, Viitanen A, et al. ImmunoRatio: a publicly available web application for quantitative image analysis of estrogen receptor (ER), progesterone receptor (PR), and Ki-67. *Breast Cancer Res*. 2010;12:R56.
28. Landini G. Colour deconvolution. 2015. Available at: http://www.mecourse.com/landinig/software/cdeconv/cdeconv.html. Accessed November 24, 2015.
29. Ihaka R, Gentleman RR. A language for data analysis and graphics. *J Comput Graph Stat*. 1996;5:299–314.
30. Cross-validation (statistics). 2015. Available at: https://en.wikipedia.org/w/index.php?title = Cross-validation_(statistics)&oldid = 685033309. Accessed November 15, 2015.
31. Sing T, Sander O, Beerenwinkel N, et al. ROCR: visualizing classifier performance in R. *Bioinformatics*. 2005;21:3940–3941.
32. Robin X, Turck N, Hainard A, et al. pROC: an open-source package for R and S+ to analyze and compare ROC curves. *BMC Bioinform*. 2011;12:77.
33. Mutterer J, Zinck E. Quick-and-clean article figures with FigureJ. *J Microsc*. 2013;252:89–91.
34. Goldstein NS, Ferkowicz M, Odish E, et al. Minimum formalin fixation time for consistent estrogen receptor immunohistochemical staining of invasive breast carcinoma. *Am J Clin Pathol*. 2003;120: 86–92.
35. Yildiz-Aktas IZ, Dabbs DJ, Bhargava R. The effect of cold ischemic time on the immunohistochemical evaluation of estrogen receptor, progesterone receptor, and HER2 expression in invasive breast carcinoma. *Mod Pathol*. 2012;25:1098–1105.
36. Bigras G, Marcelpoil R, Brambilla E, et al. Cellular sociology applied to neuroendocrine tumors of the lung: quantitative model of neoplastic architecture. *Cytometry*. 1996;24:74–82.

 